26th EPS Conf. on Contr. Fusion and Plasma Physics, Maastricht, 14 - 18 June 1999 ECA Vol.23J (1999) 273 - 276

H-mode studies using the HELIOS (HELium Injection and Optical Spectroscopy) diagnostic on COMPASS-D tokamak

A.R. Field, S.J. Fielding, P. Helander, H.R. Wilson,
J.M.A. Ashbourn[†], P.G. Carolan, P.B. Jones[*], M.G. O'Mullane[‡]

EURATOM/UKAEA Fusion Association,
Culham Science Centre, Abingdon, Oxon, OX14 3DB, UK

[†]*Mathematical Institute, Oxford University, 24-29 St. Giles', Oxford, OX1 3LB, UK*

[*]*Imperial College of Science, Technology & Medicine, London University,*
Prince Consort Road, London, SW7 2BZ, UK

[‡]*Department of Physics and Applied Physics, Strathclyde University, Glasgow, G4 ONG, UK*

Introduction:

COMPASS-D is the smallest tokamak (R = 0.56 m, a = 0.17 m) with elongated (κ = 1.6), single-null plasmas achieving clear H-modes, so it can potentially provide key scaling data for ITER-like devices. The HELIOS (HELium Injection and Optical Spectroscopy) diagnostic [1] has been developed to facilitate investigations of plasma boundary physics on this device. Electron temperatures and densities at the plasma edge are determined from ratios of the localised He I line emission from a gas jet. These measurements are available with sufficient spatial (5 mm) and temporal (1 ms) resolution to attempt detailed comparisons of edge plasma stability with theoretical predictions, e.g. for the edge-localised MHD 'peeling' mode [2]. On COMPASS-D the ECRH heating power (60 GHz, ω_{ce} at 2.14 T, $P_H \leq 1.5$ MW delivered) required to achieve H-mode increases strongly as the operating density decreases [3], in marked contrast to ITER scalings obtained predominantly from NBI heated plasmas. The peeling mode, which is stabilised by pressure gradient and destabilised by edge current density, may offer an explanation of this different scaling behaviour. Plotting data from several discharges to produce an operating diagram in the appropriate dimensionless parameter space (α, ν_e*) shows H-mode conditions to be localised to a region of this space topologically similar to that of peeling mode stability. A comparison of the observed thresholds with those predicted for the peeling mode is complicated both by uncertainties in the measurements due to the underlying atomic physics and by the range of threshold values consistent with the model assumptions. 'Benchmarking' of the measurements against other diagnostics (e.g. edge Thomson scattering) is required, as well as more detailed theoretical modelling of the absolute thresholds in order to test this hypothesis more rigorously. HELIOS data are also used to evaluate a bifurcation criterion for the underlying neo-classical ion transport, which is predicted by theory to be reduced in the presence of a steep density gradient.

Diagnostic:

Line emission from neutral helium puffed at the plasma boundary can provide localised measurements of T_e and n_e in this region. The relatively high ionisation potential of He I (24.6 eV) allows thermal helium to penetrate the edge plasma ($n_e\lambda_i \approx 10^{17}$ m^{-2} where λ_i is the ionisation length). Intensity ratios of singlet-singlet (668 / 728 nm) and singlet-triplet (728 / 706 nm) line pairs are sensitive mainly to either n_e or T_e respectively. Diagnostics based on this principle have been implemented on several devices [4, 5].

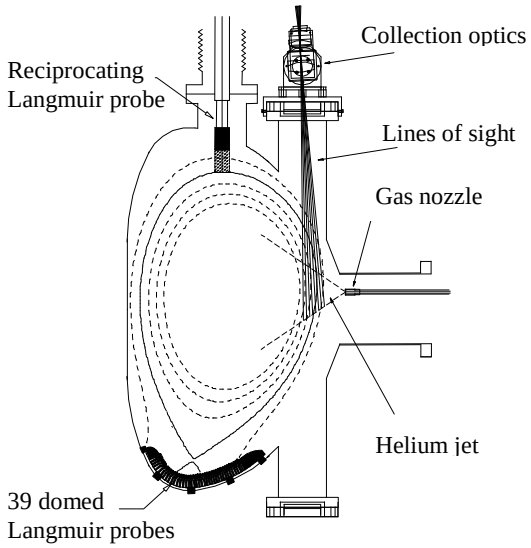

Fig. 1 Schematic of the boundary diagnostics on COMPASS-D showing the HELIOS viewing optics and gas nozzle and Langmuir probe diagnostics.

The layout of the HELIOS diagnostic on COMPASS-D, along with Langmuir probe diagnostics, is shown in Fig. 1. In the initial system thermal helium is puffed from an open, 4 mm internal-diameter tube just above the mid-plane. A steady influx of about 10^{19} s^{-1} is admitted throughout the discharge via a piezo valve. Emission from the helium jet is imaged onto an array of ten 400 μm fibres using a 100 mm, f/2 camera lens, resulting in a spatial resolution of 5 mm at the jet and a radial coverage of ≈ 50 mm encompassing the separatrix. This light is imaged at the entrance of an astigmatism-corrected, 0.6 m, f/4.5 Czerny-Turner spectrometer, fitted with a 100×100 mm^2, 300 l/mm grating, using a pair of camera lenses (50 mm:100 mm) front-to-front to match the *f*-number of the fibres to that of the spectrometer. At the exit plane a further pair of camera lenses (100 mm: 35 mm) images the focal plane onto a CCD camera [6], resulting in an inverse dispersion at the CCD of 15.6 nm / mm and a spectral coverage of 125 nm. This is sufficient to encompass the three conveniently neighbouring He I lines and D_α (656.1 nm). A filter can be inserted at the exit focal plane to attenuate this strong D_α line to optimise the dynamic range of the measurement. The cooled CCD (385 × 578, 22 μm^2 pixels) has a row transfer time of 1 μs allowing binning of charge from the regions corresponding to each chord into single rows in the store region in 300 μs. Up to 28 frames can be stored and integration times can be as short as 1 ms. Smearing due to inter-chord cross talk occurring during binning is removed numerically [1].

Values of T_e and n_e are determined from the measured intensity ratios of the 668 / 728 nm and 728 / 706 nm lines using emission coefficients for the three lines as described in [1]. These coefficients are obtained from an appropriate collisional radiative (CR) model for He I. Time independent, 0D models of the level populations are appropriate as the time scale for achieving population equilibrium is short [4]. Relaxation lengths for thermal helium (300K) scale approximately as $\lambda_r \approx 5\times10^{15}$ m^{-2} / n_e, resulting in a radial resolution of 5 mm at 10^{18} m^{-3}. We use excitation rates from the atomic data and analysis structure (ADAS) [7], which computes a full CR model for the 19 resolved *ls*-levels with principal quantum number $n \leq 4$.

The accuracy of these measurements is subject to systematic uncertainties in the emission coefficients. These coefficients are available from several collisional-radiative (CR) models [7, 8, 9, 10], which differ in the details of the atomic physics. For example, the ADAS model has recently been extended to resolve the 29 *ls*-levels with $n \leq 5$ and to use the most appropriate cross-section data following Brix [8]. Brix carried out a full error propagation of estimated uncertainties in the rate coefficient data through to the relative level populations. At T_e of 100 eV and n_e of 10^{19} m^{-3} relative uncertainties of ± 56% and ± 120% in the 668 / 728 nm and 728 / 706 nm intensity ratios respectively were computed. Because the underlying uncertainties are systematic rather than random the actual uncertainties in the ratios may be less than this, the individual uncertainties tending to cancel one another [8].

We have compared values of T_e and n_e obtained from the four different sets of coefficients with respect to those obtained using the revised coefficients from ADAS. At temperatures

above 50 eV the relative differences $\Delta T_e / T_e$ are in the range –70% to +30% and $\Delta n_e / n_e$ in the range –20% to +50%. As expected, the greatest consistency is between the revised ADAS and Brix CR models. The discrepancies between the original and revised ADAS coefficients are largest, the values of T_e obtained from the revised ADAS data being ≤ 70% below and the values of n_e ≤ 30% above those obtained using the original ADAS coefficients. The plots presented below were prepared using the original ADAS emission coefficients. However, the effect of using the revised emission coefficients for this analysis is discussed.

Results:

Theoretical calculations show that the peeling mode [2], an edge-localised, ideal MHD mode, can be unstable at low densities and could prevent the formation of an edge transport barrier. This may provide an explanation for the H-mode power threshold scaling found on COMPASS-D with ECRH heating at low operating density. The peeling mode is destabilised by edge current density and stabilised by pressure gradient, characterised by the ballooning parameter, $\alpha = -Rq^2\beta'$. It is predicted to be stable above a critical collisionality, $\nu^*_{e,cr} \approx 1$, because of reduced bootstrap current, and above a threshold pressure gradient, α_{cr} but unstable for all α at lower collisionality, defined as $\nu_e^* = \nu_{ei} / \nu_{th,e} \cdot qR / \varepsilon^{3/2}$.

The experimental α-ν^*_e operating diagram is compared with the thresholds for peeling mode stability. To accommodate changes in the plasma position, interpolated values of n_e and T_e from HELIOS at the 90% poloidal flux surface are used to determine α_e and ν^*_e for a number of L- and H-mode plasmas. It is reasonable to use the electron pressure only as, with ECRH heating it is the electrons which are heated. In Fig. 2, the measurements are classified in terms of L- and H-mode plasmas and whether an ELM occurred in the 1-2 ms integration period. H-mode plasmas are seen to occur predominantly in the peeling mode stable region of α-ν^*_e parameter space (with $\alpha \geq 0.5$, $\nu^*_e \geq 1$) consistent with this mode preventing formation of the transport barrier. In addition, ELMs are seen to occur more frequently towards the unstable region at lower collisionality and to reduce the pressure gradient to values at or below the critical value $\alpha_{cr} \approx 0.5$. The L/H-mode transitions also occur at the boundary between the L- and H-mode regions of operating space.

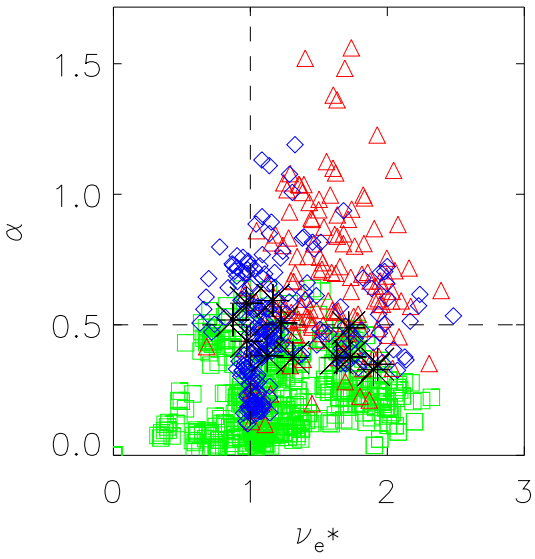

Fig. 2 Edge stability plot showing measured points at the 90% flux surface in α-ν^*_e parameter space classified according to the confinement mode (□–L-mode, Δ–ELM-free H-mode) or occurrence of ELMs (◇–H-mode with ELM). Conditions at the L/H-mode transitions are also shown (✳).

Using the revised ADAS coefficients for this analysis results in an operating diagram which is topologically similar to Fig. 1 but with α_{cr} ($\propto nT$) reduced to ≈ 0.25 and $\nu^*_{e,cr}$ ($\propto n / T^{5/2}$) increased by a factor ≈ 10. Although these changes are large, particularly for ν^*_e, it should be emphasised that there is also a significant range of threshold values from theory, depending upon the precise edge conditions. For example, the ν^*_e threshold depends upon the efficiency of de-trapping electrons (thus reducing the bootstrap current), which is determined by the edge pressure gradient, Z_{eff} and the magnetic geometry. Threshold ν^*_e values ranging from ≈

0.2 to 5 are possible, detailed modelling being required for more precise predictions. Similarly the threshold α is determined by the edge Ohmic current density, which is governed by Z_{eff}, T_e and the loop voltage, again with significant uncertainty possible.

An extension to neo-classical theory to allow for steep gradients [12] predicts that a reduction in the underlying ion transport, which is driven by ion-impurity friction, should occur at sufficiently steep density gradient. Such a reduction may occur during the H-mode. The transition criterion is characterised by the parameter

$$g_{neo} = -Z_I^{\,2} qR/\Omega_i \tau_{ii} \,(d\ln n_i/dr - 0.5\, d\ln T_i/dr),$$

where Z_I is the charge state of the dominant impurity. When g_{neo} exceeds a value ≈ 1 a reduction in ion transport might be expected. Fig. 3 shows a plot of HELIOS edge data in (g_{neo}, ν^*_e) parameter space (where it is assumed that T_i / T_e = n_i / n_e = 1 and Z_I = 5) indicating that H-mode occurs above a threshold value of g_{neo} in the range 0.2 to 0.4. The observed threshold increases with ν^*_e as predicted by theory, since the ratio of edge ion to electron temperature might be expected to increase at higher collisionality. If revised ADAS data are used for this analysis the g_{neo} ($\propto n / T^{3/2}$) increase by a factor ≈ 7 and ν^*_e by a factor ≈ 10. Again, the theoretical threshold also has a large uncertainty due to our use of electron rather than the appropriate ion parameters and the uncertainty of the dominant ion charge state.

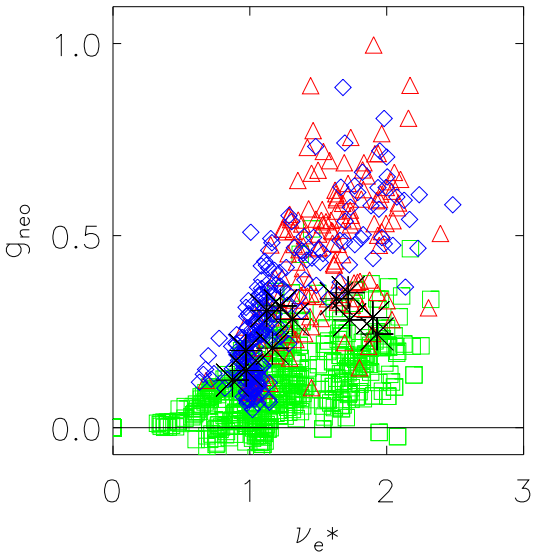

Fig. 3 Edge data at the 90% flux surface in g_{neo}-ν^*_e parameter space classified according to the confinement mode (□–L-mode, Δ–ELM-free H-mode) or occurrence of ELMs (◇–H-mode with ELM) and L/H-transitions (✳).

In conclusion, the peeling mode offers a possible explanation of the H-mode power threshold scaling with ECRH heating found on COMPASS-D, this mode perhaps preventing formation of the edge confinement barrier at low density. H-mode is observed to be restricted to a region of (α-ν^*_e) space topologically similar to that where this mode is stable. However, a quantitative comparison of stability thresholds to confirm these ideas awaits more detailed theoretical modelling and benchmarking of HELIOS measurements against other edge diagnostics. HELIOS data has also been used to show that a possible reduction in the underlying neo-classical ion transport may occur under COMPASS-D H-mode conditions.

References:

[1] A. R. Field, N. J. Conway, P. G. Carolan, M. G. O'Mullane, Rev. Sci. Inst., **70**, 1 (1999).
[2] J. W. Connor, R. J. Hastie, H. R. Wilson, R. L. Millar, Phys. Plasmas **5** (1998) 2687.
[3] S. J. Fielding et al., Plasma Phys. Contr. Fusion **40** (1998) 731.
[4] B. Schweer, G. Mank, A. Pospieszczyk, B. Brosda, B. Pohlmeyer, J. Nucl. Mater. **196-198** (1992) 174.
[5] S. J. Davis et al,. J. Nucl. Mater. **241-243** (1997) 426.
[6] Wright Instruments Ltd., Unit 10, 26 Queensway, Enfield, Middlesex, EN3 4SA, UK.
[7] H.P. Summers, '*Atomic data and analysis structure*', JET Report, JET-IR (94) 06, 1994.
[8] M. Brix, Ph.D. Thesis, Rühr-Universität, Bochum, 1998.
[9] P. Kornejew, Ph.D. Thesis, Humboldt-Universität, Berlin, 1996, IPP-Report, IPP-8/10, 1996.
[10] M. Goto, T. Fujimoto, NIFS Research Report, NIFS-DATA-43, 1997.
[11] B. N. Rogers, F. L. Drake, Phys. Rev. Letters, **79**, 2 (1997) 229.
[12] P. Helander, Physics of Plasmas, **5**, 11 (1998) 3999.

This work is funded jointly by the UK Department of Trade and Industry and EURATOM.